*Proceedings of the 16th International Conference on Soil Mechanics and Geotechnical Engineering*

*doi:10.3233/978-1-61499-656-9-2673*

# Effects of irregular dynamic loads on soil liquefaction

## Effets des charges dynamiques irrégulières sur le sol de liquéfaction

S.I. Kim, K.B. Park, S.Y. Park, S.J. Hwang, & J.H. Lee
*Dept. of Civil Eng., Yonsei University, Seoul, Korea*
J.S. Choi
*Disaster Prevention Research Institute, Kyoto University, Uji, Japan*

ABSTRACT
The sinusoidal types of cyclic loading have been commonly used for investingating dyamic responses of soils under earthquake loading, primarily due to simplicity. In this study, dynamic triaxial tests with different types of dynamic loadings including sinusoidal, triangular, incremental, and 9 real earthquake loadings were performed to investigate effects of loading type on liquefaction behavior. Based on test results, mobilization of the excess pore water pressure and the deviatoric stress is analyzed and compared. The phase transformation line from the effective stress path is introduced and investigated for generation of initial liquefaction. Stress damage concept based on the stress-time history and the cumulative energy is addressed and investigated as well.

RÉSUMÉ
Les types sinusoïdaux de chargement cyclique ont généralement utilisé pour investingating des réponses dyamic des sols dessous chargement de tremblement de terre, principalement dû à la simplicité. Dans cette étude, essais à trois axes dynamiques avec différents types de chargements dynamiques comprenant des chargements sinusoïdaux, triangulaires, par accroissement, et 9 vrais de tremblement de terre ont été effectués pour étudier des effets de charger le type sur le comportement de liquéfaction. Basé sur l'essai résultats, mobilisation de la pression excessive d'eau interstitielle et le deviatoric l'effort est analysé et comparé. La phase transformation ligne du chemin efficace d'effort est présenté et étudié pour la génération de la liquéfaction initiale. Effort le concept de dommages basé sur l'histoire de soumettre à une contrainte-temps et l'énergie cumulative est adressé et étudié aussi bien.

## 1 INTRODUCTION

Most liquefaction analysis using cyclic test results have been in general based on the equivalent shear stress concept proposed by Seed and Idriss (1971). At the same time, it is also known that the sinusoidal type of cyclic loadings does not realistically represent actual irregular earthquake motions. While some model tests with real earthquake motions using the shaking table and other laboratory devices were carried out in Japan and U.S.A., those were primarily for simulation and verification of specific local liquefaction hazards. Although application of irregular motions would be more realistic for actual seismic analysis, it requires complex testing systems and significant amount of time and efforts. Recently, various dynamic testing systems, which can simulate user-defined irregular motions, were introduced and have made it more effective to analyze dynamic responses of soils under real earthquake motions.

In this paper, a series of dynamic tests were performed using different types of dynamic loads including sinusoidal, triangular, incremental, and real earthquake motions. Based on test results, dynamic responses of soils under regular and irregular real earthquake motions are analyzed and compared. For the determination of initial liquefaction, the phase transformation line obtained from the effective stress path is introduced and investigated. Stress damage concept based on the stress-time history and the cumulative energy obtained from the stress-strain curves are addressed and investigated as well.

## 2 INITIAL LIQUEFACTION

Choi and Kim (2003) experimentally verified that the liquefaction initiation is related to the phase transformation line (PTL), which is determined from the effective stress path. It was also proposed that the dynamic responses of sands can be divided into following three different stages; ① the gradual degradation, ② the rapid degradation and liquefaction initiation, and ③ the post liquefaction. This is illustrated in Fig. 1. Results by Choi and Kim (2003) indicate that the initial liquefaction occurs when the effective stress path reaches the PTL with dramatic changes in the pore water pressure and deformation. It should be noticed that, however, these observations were obtained from test results using regular sinusoidal loadings.

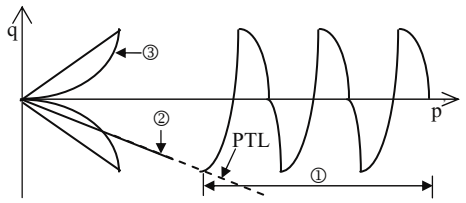


Figure 1. Dynamic soil state (Choi and Kim, 2003)

Waveforms of the deviatoric stress in soils induced by actual earthquake loadings are irregular. Liquefaction potential for sands subjected to irregular waveforms of deviatoric stress, therefore, cannot be defined in the same manner as that for regular sinusoidal loadings. According to the shape of the waveform, earthquake loadings can be categorized as impact and vibration types (Ishihara and Yasuda, 1975). While this classification is simple and useful for the evaluation of liquefaction potential, it does not reflect other significant dynamic factors such as the number of loading cycles and motion of duration in detail for irregular real earthquake motions.

## 3 DYNAMIC LABORATORY TEST

In order to investigate effects of irregular earthquake loadings on dynamic soil characteristics, 9 acceleration records were collected from an available website (http://db.cosmos-eq.org), and used in dynamic laboratory tests. Collected earthquake records are summarized in Table 1. In Table 1, the duration indicates the significant durations (Trifunac and Brady, 1975), which is

the 5-95% RMS (Root-Mean-Square) duration. The earthquake types defined in Table 1 were classified based on the criterion proposed by Ishihara and Yasuda (1975). According to Ishihara and Yasuda (1975), the impact type earthquake is the one with one or two high amplitudes greater than 60% of the maximum peak amplitude prior to the maximum peak while the vibration type is the one with high amplitudes of more than 3 occurrences.

The dynamic testing system employed in this study allows the maximum frequency equal to 70 Hz of dynamic loading. Parameters measured from tests include axial deformations, volume changes, deviatoric stresses, and pore water pressures, all of which were recorded with time. The testing system used in this study can also apply different types of cyclic loadings such as sinusoidal, triangular, and various user-defined irregular motions. Test soil is the Jumunjin sand, a representative silica sand in Korea. Fundamental laboratory tests were also performed to determine various geotechnical properties including the grain size distribution, the specific gravity ($G_s$), and the maximum and minimum void ratios ($e_{max}$ and $e_{min}$). All tests were performed following ASTM specifications. Test results and basic properties of the Jumunjin sand are given in Table 2. Triaxial soil samples used in this study are of 70 mm in diameter and 140 mm in height. The water sedimentation method was adopted for sample preparations as described in Kim (2004). The test samples were saturated by applying back-pressure and kept until the B parameter exhibits 0.97 or greater. All the samples were then allowed to be isotropically consolidated at a confining pressure equal to 100 kPa for more than 1 hour.

Fig. 2 shows four different types of cyclic loadings used in the tests; sinusoidal, triangular, incremental, and irregular real earthquake loadings. In particular, tests with incremental and irregular earthquake loadings were repeated until initial liquefaction occurs by increasing the peak stress incrementally. For the incremental loading [Fig. 2 (c)], tests were also repeated using different $\Delta t$ (1.0 sec. and 0.2 sec.) and slopes (n) [i.e., $n_1$, $n_2$, and $n_3$ in Fig. 2(c)] prior to the maximum peak deviatoric stress.

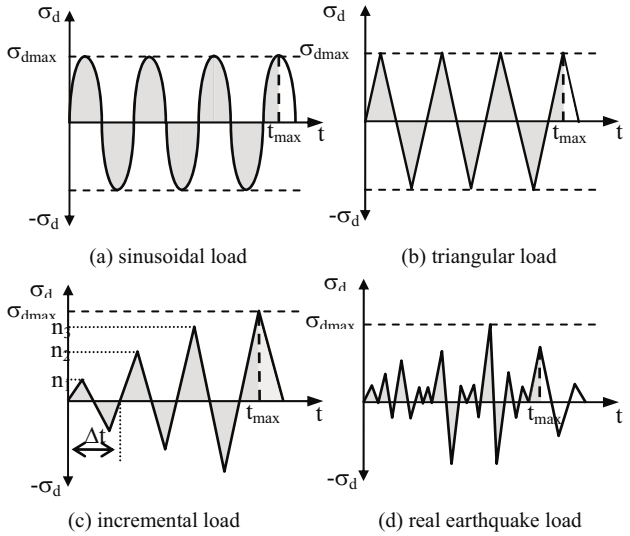


Figure 2. Types of dynamic load used in this study

Table 1. Collected earthquake records (http://db.cosmos-eq.org)

| Earthquake | Type | Moment magnitude | Duration |
|---|---|---|---|
| Parkfield | Impact | 6.1 ($M_w$) | 24.0 sec |
| Ormond | Impact | 6.2 ($M_w$) | 20.0 sec |
| Cass | Vibration | 6.2 ($M_w$) | 10.0 sec |
| Baja California | Vibration | 6.4 ($M_w$) | 18.0 sec |
| Big Bear | Impact | 6.5 ($M_w$) | 22.0 sec |
| Taumaranui | Impact | 6.6 ($M_w$) | 20.0 sec |
| El-Centro | Vibration | 7.1 ($M_w$) | 24.0 sec |
| Costa-Rica | Impact | 7.5 ($M_w$) | 21.0 sec |
| Michoacan | Vibration | 8.1 ($M_w$) | 23.0 sec |

Table 2. Properties of soil tested

| $G_s$ | $e_{max}$ | $e_{min}$ | $D_{50}$ | $C_u$ | $C_c$ |
|---|---|---|---|---|---|
| 2.63 | 0.885 | 0.638 | 0.52 mm | 1.35 | 1.14 |

* $D_{50}$ : average grain size.
$C_u$ & $C_c$ : coefficient of uniformity and curvature

## 4 RESULTS OF DYNAMIC TESTS

Based on test results using 9 earthquake records and 3 loading shapes shown in Fig. 2, various dynamic soil responses, including the deviatoric stress and the PWP, were analyzed. In the analysis, as this study focuses on liquefaction initiation under different loading types, following 2 significant components were selected and investigated; mobilization of the PWP and stress damage ratios in terms of cumulative energy up to liquefaction initiation defined from the PTL in Fig. 1. The calculation of cumulative energy and stress damage ratios will be further discussed in later section.

Figs. 3, 4, and 5 show mobilization of the PWP with time for different types of dynamic loadings. Test results with sinusoidal and triangular loadings are given in Figs. 3(a) and (b). From the figure, it is observed that the PWP builds up gradually with time and eventually reaches a value equal to the initially applied confining pressure for both types of regular cyclic loadings. It is also seen that the higher the maximum deviatoric stress, the lesser the time to reach the liquefaction initiation point. On the other hand, in the case of irregular loadings with incremental motions, liquefaction is observed to occur at a certain point where a dramatic increase of the PWP is generated [see Figs. 3(c) and (d)]. Consequently, the PWP build-up curves for incremental loadings appear to be quite different from those for regular cyclic loadings. As indicated in Figs. 3(c) and (d), significant factors for the liquefaction initiation are the time increment $\Delta t$ and the stress slope n. It is observed that initial liquefaction occurs faster with $\Delta t$ = 0.2 sec than with $\Delta t$ = 1.0 sec. As a result, stress slope n increases as the liquefaction initiation time decreases. It was also found that results of PWP mobilization shown in Figs. 3(c) and (d) represent similar trends to those obtained from tests using real earthquake loadings in Figs. 4 and 5. It can be, therefore, concluded that PWP mobilization and thus liquefaction initiation in irregular loading cases differ from those in regular cyclic loading cases. This also indicates that the conventional approach using regular cyclic loading may not sufficiently represent detailed dynamic responses of soil under actual earthquake loadings.

In Figs. 4 and 5 for Parkfield and Taumaranui earthquakes, the maximum deviatoric stresses corresponding to the initial liquefaction occurred at +36.2 kPa and –33.7 kPa, respectively. Based on loading shape and dynamic soil responses obtained in this study, types of earthquake are classified into two different groups: blazing and terraced types. The blazing type of earthquake is similar to the impact type where the maximum peak loading is main factor for the liquefaction initiation. On the other hand, the terraced type of earthquakes represents earthquake loadings where the liquefaction initiation is governed by the maximum peak loading point as well as post-peak loadings of significant amplitudes. The blazing type includes Parkfield (Fig. 4), Cass, Big Bear, El-Centro, and Costa-Rica earthquakes while Taumaranui (Fig. 5), Ormond, Baja California, and Michoacan earthquakes are the terraced type. As shown in Fig. 4 of the blazing type, the initial liquefaction is observed to occur around the peak amplitude as marked with black circles. In this case, the peak load signal produces the remarkable increase of the PWP and the PWP is preserved before liquefaction is fully driven by the following stress. For the terraced type shown in Fig. 5, a terrace is observed after the peak loading marked with black circle before initial liquefaction. From these results, it is reconfirmed that the most important factor to drive initial liquefaction is the peak signal of earthquake motion. However, for the case where the following loading levels after peak are con-

siderably high, it is observed that the subsequent loadings after peak can also produce significant PWP jump.

In conventional cyclic triaxial tests, soil samples are in general loaded with sinusoidal deviatoric stresses at an appropriate cyclic stress ratio until they liquefy. For irregular earthquake motions, however, unlike the sinusoidal loading case, it is necessary to evaluate a magnitude of stress, at which liquefaction is first generated, by repeating tests using the same earthquake motion with varying acceleration levels. As shown in Figs. 3(a) and (b), cyclic triaxial test results using regular loadings show that the pore water pressure builds up gradually as the number of cyclic stress increases, and eventually reaches a value equal to the initially applied confining pressure. For irregular earthquake loadings shown in Figs. 4 and 5, in particular for the impact or blazing type, it is noted that the pore pressure does not increase in earlier stages, but suddenly jumps up when the maximum deviatoric stress is reached, whereupon liquefaction sets in.

In order to analyze effects of real earthquake motions to change the PWP, deviatoric stresses to drive the remarkable increase of the PWP were investigated in detail. Fig. 6 shows deviatoric stress ratios versus pore pressure ratios at individual peak points [e.g., stresses at $n_1$, $n_2$, $n_3$ in Fig. 2(c)] when the PWP ratio is greater than 0.1 (i.e., over 10 kPa).

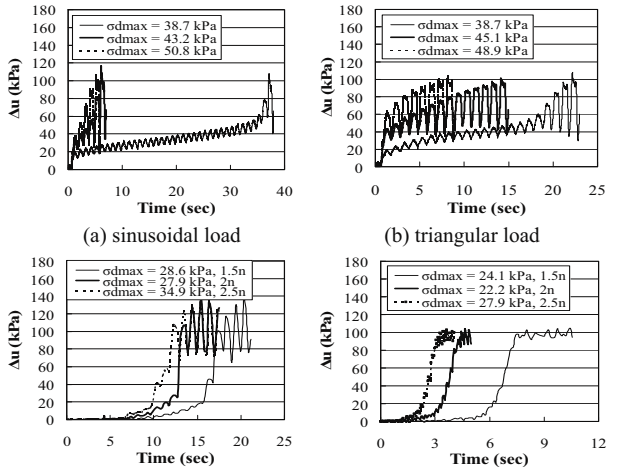


(a) sinusoidal load (b) triangular load

(c) incremental load (Δt = 1 sec) (d) incremental load (Δt = 0.2 sec)

Fig. 3 Typical time histories curves of the excess pore water pressure

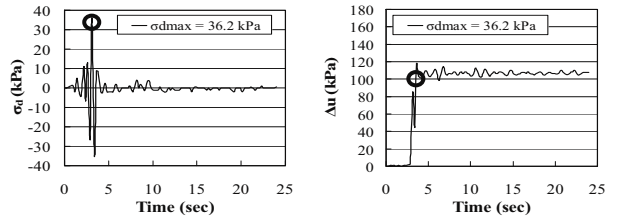


(a) applied deviatoric stress curve (b) pore water pressure curve

Fig. 4 Example of the first type earthquake (Parkfield)

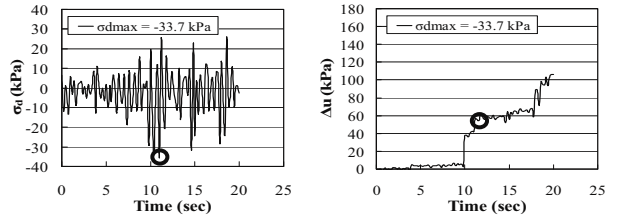


(a) applied deviatoric stress curve (b) pore water pressure curve

Fig. 5 Example of the second type earthquake (Taumaranui)

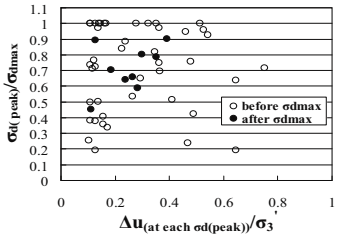


Fig. 6 Peak deviatoric stress ratio and PWP ratio generated at the peak deviatoric stress ratio

As shown in Fig. 6, stress ratio points affecting the remarkable change of PWP before the peak loading were located in various levels but points after peak loading were marked in the high level over stress ratio greater than 0.5. This result confirms that both the maximum peak and post-peak loadings are important for the generation of liquefaction. While Ishihara and Yasuda (1975) proposed types of earthquakes as a function of the number of the high stresses prior to the maximum peak, results obtained in this study indicate that post-peak loadings should also be taken into account for more realistic and detailed classification of earthquakes. Accordingly, classification into the blazing and terraced types is believed to be more appropriate than that into impact and vibration types by Ishihara and Yasuda (1975). This in turn raises a need to establish a proper criterion on amplitudes of post-peak loadings to initiate the subsequent liquefaction for the terraced type.

## 5 STRESS DAMAGE RATIO

As discussed previously, the liquefaction resistance strength for real earthquake loading may differ from that obtained from a laboratory test using the sinusoidal loading (Kim, 2004). It is also difficult to compare directly results from sinusoidal with those from real earthquake loadings. In order to establish more effective classification for various dynamic loadings, a new stress-time history parameter (called stress damage ratio in this study), κ, is introduced and defined as follows:

$$\kappa = \frac{1}{T_{max} \cdot \sigma_{d\,max}} \left( \sum_{0}^{T_{max}} |\sigma_d \cdot t| \right) \tag{1}$$

where t = time; and $T_{max}$ = time until the liquefaction initiation. As illustrated in Fig. 2, the summation in Eq. (1) represents the entire shaded areas. During the impulse load, the soil is subjected to the maximum deviatoric stress for a very short time, and hence κ value is nearly equal to zero. For the perfectly square shape, the soil is subjected to the maximum deviatoric stress for entire period $T_{max}$, and hence κ is equal to 1. It can be seen that κ is defined for given $\sigma_{dmax}$ and $T_{max}$ in such a way that it increases if the soil is subjected in one cycle to higher stresses for longer liquefaction time. Therefore, it is seen that the higher the κ value, the greater the external force (i.e., summation of deviatoric stress with time) acting on the soil until initial liquefaction.

In order to confirm the proposed parameter κ, values of κ are compared with the cumulative energy. The cumulative energy can be computed from the area that is defined from the stress-strain curve. The expression for cumulative energy per unit volume, w(t), is given by:

$$w(t) = \sum_{0}^{T_{max}} \sigma_{ij} d\varepsilon_{ij} \tag{2}$$

where $T_{max}$ = time until liquefaction initiation; $\sigma_{ij}$ = stress vector; and $\varepsilon_{ij}$ = strain vector.

In this study, the initial liquefaction point was defined based on the phase transformation line (PTL) approach. According to Choi and Kim (2003), the calculation of the liquefaction resistance index includes most of large deformation data in terms of

strains, indicating a close relationship between liquefaction resistance and cumulative energy given by (2). Fig. 7 shows effective stress paths and the angle of the PTL for sinusoidal and Taumaranui earthquake loadings. As shown in Fig. 7, the effective stress paths clearly exhibit reversal points from contractive to dilative stages as the stress paths approach to the PTL. It is also seen that the dilative response (i.e., rapid degradation stage in Fig. 1) after touching PTL appears to occur near the condition of liquefaction. In this study, the PTL was obtained from the start point of the rapid degradation with high pore pressure ratios greater than 0.5. The angle of PTL was found to be approximately 26.5° for all the tests. The angle of PTL equal to 26.5° is in reasonable agreement with the angle of 28.6° estimated from laboratory static tests obtained by Kim (2004).

Figs. 8 (a) and (b) show values of κ with the maximum deviatoric stress and cumulative energy respectively. In Fig. 8, sinusoidal and triangular loads show approximately κ = 0.66 and 0.55 respectively, while incremental and real earthquakes show κ = 0.20 – 0.31 and κ = 0.11 – 0.26 respectively. For sinusoidal and triangular loadings, values of κ are higher than those of incremental and earthquake loadings, as amount of overall input stress is greater. All cumulative energies calculated from irregular loading tests are not over 100 J/m$^3$ while those from cyclic loads are over 100 J/m$^3$. These results indicate that determination of liquefaction occurrence using cyclic loadings may result in overestimation since tests using cyclic loadings are associated with bigger cumulative energy than those for actual earthquake loadings.

Fig. 9 summarizes results for the cumulative energy developed by sinusoidal, triangular, incremental, and real earthquake loadings for a constant κ value. The figure clearly shows that the larger the maximum deviatoric stress, the smaller the cumulative energy until liquefaction initiation for the same κ value. This is because time required to initiate liquefaction for higher deviatoric stress is shorter than that for lower deviatoric stress. For similar κ values, magnitudes of cumulative energy for sinusoidal and triangular loadings, marked with squares in Fig. 9, are quite different from those for irregular loadings. On the other hand, results from incremental loading tests appear to be similar to those of earthquake loading tests. From Fig. 9, it is seen that the cumulative energy until liquefaction initiation decreases with increasing maximum deviatoric stress. It is also seen that the decrease of the cumulative energy with maximum deviatoric stress becomes more pronounced as values of κ increase. Based on this observation, it can be concluded that the κ can be used as an effective parameter for the classification for shape of dynamic loadings.

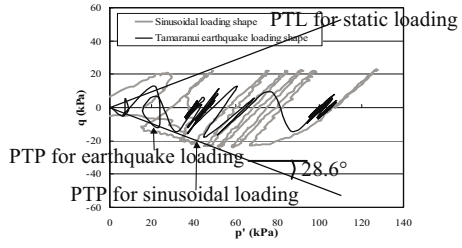


Fig. 7 Comparison on angles of PTLs

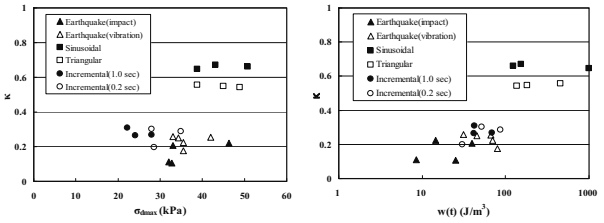


(a) (b)

Fig. 8 Comparison on κ with maximum deviatoric stress and cumulative energy

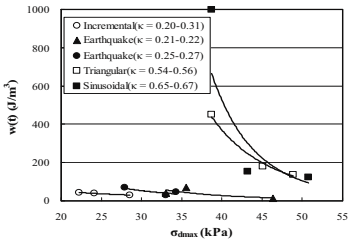


Fig. 9 Cumulative energy versus maximum deviatoric stress

## 6 SUMMARY AND CONCLUSIONS

A series of dynamic loading tests was performed to investigate dynamic responses of soil and liquefaction behavior under various loading types. Based on test results, detailed dynamic responses of soils, including mobilization of excess pore water pressure, deviatoric stress, and effective stress path under regular and irregular real earthquake motions were compared and analyzed. Stress damage concept based on the stress-time history and the cumulative energy obtained from the stress-strain curves were also introduced and investigated for different types of dynamic loadings.

From the test results, it was found that cyclic loading tests with sinusoidal and triangular signal do not accurately simulate dynamic responses of soil under real earthquake loadings. From results of mobilization of excess pore water pressure and initial liquefaction, a new classification of earthquake motions into blazing and terraced types was proposed. For the blazing type, the initial liquefaction occurs near the maximum peak load. For the terraced type, on the other hand, subsequent loadings of high amplitudes after the maximum peak loading point were also important consideration for the initiation of liquefaction.

From the investigation of the cumulative energy and stress damage ratio, it is confirmed that the use of the cyclic loading for seismic analyses may not be effective and likely to result in overestimated input motions. The dynamic loading tests with incremental loading shapes were observed to reflect relatively well the effect of real earthquake loading shape compared to sinusoidal loadings.

## ACKNOWLEDGEMENTS

The research herein was performed under Grant No.R11-1997-045-13003 from Korea Earthquake Engineering Research Center (KEERC). A part of this work was supported by the Post-doctoral Fellowship Program of Korea Science & Engineering Foundation (KOSEF).

## REFERENCES

Choi, J.S. and Kim, S.I. 2003. Application of disturbed state concept for the dynamic behaviors of fully saturated soils. *Proceeding of 2003 Spring-Conference of EESK*, Seoul, 7(1), 140-147.

Ishihara, K. and Yasuda, S. 1975. Sand liquefaction in hollow cylinder torsion under irregular excitation, *Soils and Foundations*, 15(1), 45-59.

Kim, S. I. 2004. Liquefaction potential in moderate earthquake regions. *12th Asian Regional Conf. on Soil Mechanics & Geotechnical Engineering*, Leung et al. (eds), World Scientific Publishing Co., 2, 1109-1138.

Seed, H.B. and Idriss, I.M. 1971. Simplified procedure for evaluating soil liquefaction potential. *J. Geotech. Engrg. Div.*, ASCE, 97(9), 1249-1273.

Trifunac, M.D. and Brady, A.G. 1975. A study of the duration of strong earthquake ground motion. *Bulletin of the Seismological Society of America*, 65, 581-626.

Vucetic, M., Lanzo, G., and Doroudian, M. Effect of the shape of cyclic loading on damping ratio at small strains. *Soils and Foundations*, 38(1), 111-120.